Materials Sciences and Applications, 2011, 2, 1688-1696
doi:10.4236/msa.2011.211225 Published Online November 2011 (http://www.SciRP.org/journal/msa)

Structural and Optical Properties of Li^+: PVP & Ag^+: PVP Polymer Films

Kothapalle Sivaiah*, Koramala Naveen Kumar, V. Naresh, Srinivasa Buddhudu

Department of Physics, Sri Venkateswara University, Tirupati, India.
Email: *ksiva.phy@gmail.com

Received September 6th, 2011; revised October 18th, 2011; accepted October 31st, 2011.

ABSTRACT

PVP polymers containing Li^+ or Ag^+ Ions have been synthesized in good stability and transparency by using the solution casting method. Their structural, optical, thermal and electrical properties have been investigated from the measurement of XRD, FTIR, SEM, EDAX, optical absorption spectra, TG-DTA profiles and impedance spectral features in order to evaluate their potentialities for their use in electrochemical display device applications.

***Keywords*:** *PVP Polymer Films-Characterization*

1. Introduction

Conducting polymers are nowadays considered to be more important in the development several applications involved polymer devices [1]. Among the many polymers, the polyvinylpyrrolidone (PVP) has good film-forming and adhesive behavior on many solid substrates and its formed films exhibit good optical quality (high transmission in visible range), and mechanical strength (easy processing) required for applications. The amorphous structure of PVP also provides a low scattering loss, which makes it as an ideal polymer for composite materials for different applications. PVP is easily soluble in water, so it is preferred to avoid phase separation in the reactions [2-4]. In literature, alkali ions containing polymers are reported to be more promising possessing potential applications [5,6]. PVP polymers have been found to be different in their functionalities from other polymeric systems, such as the PEO, PPO, PVDF, PANI, etc [7]. Like the Li^+ ion, Ag^+ ion has also drawn more attention because of its possessing potential uses in electronics, optical filters, conducting adhesives, and in the development of catalysts [8-11]. Keeping in view, the significant importance demonstrated by dopant Li^+ or Ag^+ ions in polymer films, in the present work, we have undertaken a couple of polymer films of Li^+: PVP and Ag^+: PVP alongside the host PVP polymer films, in order to understand their structural, optical and dielectric properties.

2. Experimental Studies

PVP (PolyVinylPyrrolidone) $(C_6H_9ON)_n$, chemical with a molecular weight [MW] of 1,300,000) and also two other salts of $LiNO_3$ and $AgNO_3$ salts were purchased from M/S Sigma-Aldrich Company, Hyderabad.

PVP was dissolved in a small beaker of 50 cc containing double distilled water and it was then thoroughly mixed by using a magnetic stirrer in a warmer condition for homogeneous mixing. Later, this solution was cast into polymer films in flat based Petri dishes under a slow evaporation method. Thus clearer and highly transparent host PVP film was successfully obtained. Lithium Nitrate ($LiNO_3$) and Silver Nitrate ($AgNO_3$) salts were separately dissolved in beakers containing double distilled water, PVP was mixed in double distilled water in another beaker. In 1:9 ratio; *i.e.*, solutions in 1 part of $LiNO_3$ or $AgNO_3$, 9 parts of PVP solutions were thoroughly mixed using a magnetic stirrer. All the polymer films were found to be 6 cm in diameter and from such big sized films; required sizes of films were appropriately cut for carrying out the measurements.

Figure 1(a) shows the Borosilicate containers with the solutions of the 1). Host PVP, 2). Li^+: PVP and 3). Ag^+: PVP and in **Figure 1(b)**, those solutions in polymer films are shown. Silver particles exhibit yellowish brown color in aqueous solution due to excitation of surface plasmon vibrations in silver particles [12,13]. The absorption spectra of the host PVP, Li^+: PVP and Ag^+: PVP were carried out at the room temperature on a JASCO UV-VIS -NIR spectrophotometer (Model V-570) in the wave-length range from 250 nm to 750 nm. The X-ray diffraction studies of these films were performed by means of SEIFERT

(a)

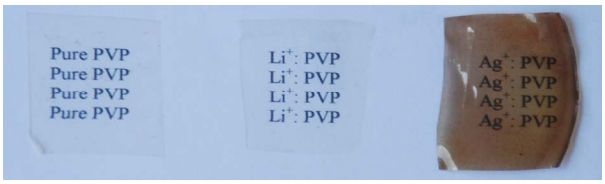

(b)

Figure 1. (a) Host PVP, Li^+: PVP and Ag^+: PVP polymer solutions; (b) Host PVP, Li^+: PVP and Ag^+: PVP polymer films.

3003TT X-ray diffractometer in the 2θ range of 5˚ - 80˚. The FT-IR spectra of host PVP and Li^+: PVP and Ag^+: PVP polymer films were rerecorded on EO-SXB IR spectrometer in the range of 4000 cm^{-1} - 500 cm^{-1}. The morphologies of the polymer films were examined on a ZEISS EVO MA15 Scanning Electron Microscope (SEM). The samples were gold coated using a sputter coater polaron SC 7610 system. The elemental analysis of these synthesized polymer films were carried out on an EDAX (INCA pentaFETx3) that is an attachment to the SEM system. Thermo gravimetric (TG) and Differential thermal analysis (DTA) simultaneous profiles were obtained for the as synthesized sample in N_2 atmosphere at a heating rate of 10˚C/min on Netzsch STA 409 Simultaneous Thermal Analyzer. The impedance measurements were carried out on computer controlled Phase Sensitive Multimeter (PSM 1140) in the frequency and temperature ranges of 1 Hz - 1 MHz and 303 - 373 K respectively.

3. Results and Discussion

3.1. Absorption Spectra Analysis

Figure 2(a), **(b)** & **(c)** show the UV-Visible absorption spectra of PVP, Li^+: PVP and Ag^+: PVP polymer films. This is in good agreement with the size distribution measurement of pure-PVP and Li^+ PVP aggregates [14]. PVP is a hydrophobic polymer which has an affinity towards the Ag^+ ion silver in the formation of covalent bond between pyridyl groups and silver ion. In **Figure 2 (c)**, there are two absorption bands at 297 nm and another at 437 nm and the band at 297 nm has been labeled to the NO_3 ligand of the Ag cation and the other one at 437 nm is attributed to the surface plasma resonance phenomena of free electrons in the conduction bands of Ag particles and absorption profiles are in accordance with the reports already made in literature for Ag^+ doped in other types materials [15,16].

3.2. XRD Analysis

The XRD patterns of the host PVP, Li^+: PVP and Ag^+: PVP polymer films are shown in **Figures 3(a)**, **(b)** & **(c)**. The XRD pattern (**Figure 3(a)**) of PVP has revealed a couple of broad bands located at 2θ = 11˚ and 22˚ respectively those could clearly indicate the amorphous nature of the host PVP [17]. However, the Li^+: PVP and Ag^+: PVP have exhibited a two-phased structural pattern, as shown in **Figures 3(b)** & **(c)** confirming both the amor-

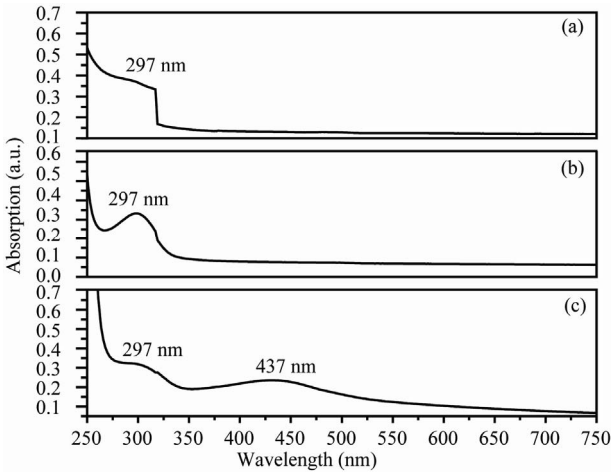

Figure 2. Absorption spectra of (a) Host PVP; (b) Li^+: PVP and (c) Ag^+: PVP polymer films.

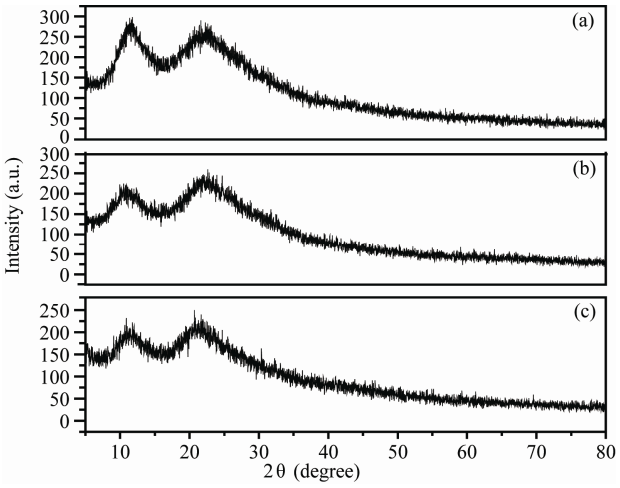

Figure 3. XRD patterns of (a) Host PVP; (b) Li^+: PVP and (c) Ag^+: PVP polymer films.

phous nature in the hexagonal and face-centered cubic (fcc) phase of lithium and silver [18].

3.3. FTIR Analysis

Figures 4(a), **(b)** & **(c)** show the FTIR spectra of the host PVP, Li^+: PVP and Ag^+: PVP polymer films. From the host PVP polymer film (curve (a)), the band relating to the pyrrolidone C=O group is located at 1698 cm^{-1}. The vibrational band at 1698 cm^{-1} corresponds to C=O stretching of PVP polymer film, C-H asymmetric stretching of CH_2 absorption band located at 2987cm^{-1}. In the case of the host PVP and it found at 2992 cm^{-1}, 2994 cm^{-1}, and 3001 cm^{-1} in the Li^+: PVP and Ag^+: PVP polymer films. The bands at 931 cm^{-1}, 1260 cm^{-1} and 1427 cm^{-1} are attributed to C-C stretching vibration, C-N stretching vibration and C-H bending vibration of host PVP respectively. Based on its absorption spectra, it is noticed that the $AgNO_3$ in the matrix studied becomes reduced and thus the absorption band is assigned to NO_3, as shown in curve (c), which disappears, and the C=O peak 1698 cm^{-1} appears due to a littler broadening [19, 20]. The peaks at 739 cm^{-1}, 2009 cm^{-1} and 2920 cm^{-1} correspond to $LiNO_3$ and $AgNO_3$ and a new peak at 1127 cm^{-1} in the complex formed PVP. The appearance of new peaks along with changes in existing peaks in IR spectra is a direct indication of the complexation of PVP with Li^+ and Ag^+ ions [21].

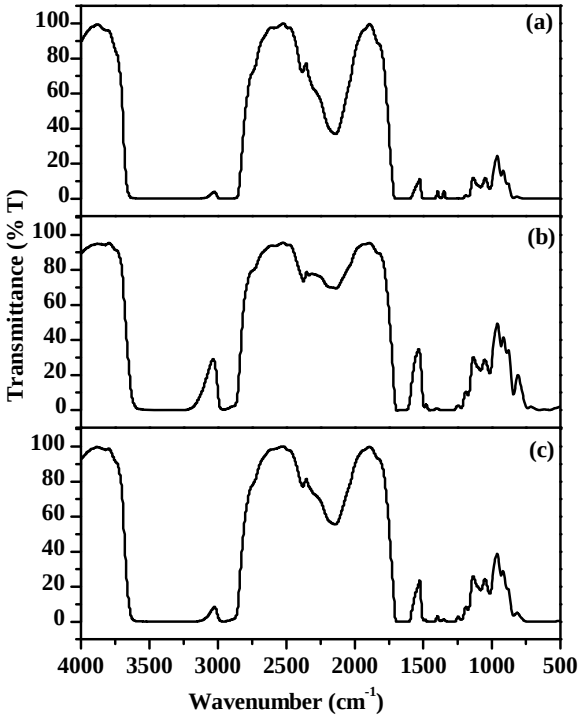

Figure 4. FTIR spectra of (a) Host PVP; (b) Li^+: PVP and (c) Ag^+: PVP polymer films.

3.4. SEM and EDAX Analysis

SEM Micrographs of the host PVP, Li^+: PVP and Ag^+: PVP polymer films are shown in **Figures 5 (a)**, **(b)** & **(c)**. The surface deposited polymer films are clearly seen at high magnification in the micrographs. **Figure 5(a)** shows the smooth surface morphology is closely related to the amorphous nature. **Figure 5(b)** shows an irregular particle appearance owing to the polymer film formation. The smooth morphology is closely related to the amorphous nature of the polymer electrolyte films. **Figure 5(c)** shows the SEM micrographs of the silver particles are spherical shaped, well distributed without aggregation in solution with an average size of about 3 μm. Both the polymer films of EDS spectrum denotes a signal observed from the silver ions [22]. To verify the chemicals in the material, an EDAX profile has also been recorded as shown in **Figures 5(d)**, **(e)** & **(f)**. However, the EDAX of the matrix to confirm the presence of C, O and Ag ions in the prepared films [23].

3.5. TG-DTA Analysis

Figures 6(a), (b) & **(c)** show the TG-DTA curves of host PVP, Li^+: PVP and Ag^+: PVP Polymer Films. The TGA thermograms of **Figures 6(a)**, **(b)** & **(c)** show the weight loss as a function of the temperature for the host PVP, Li^+: PVP and Ag^+: PVP precursor with a heating rate of 10°C/min in the temperature range from 40˚C to 600˚C. It is clear that the initial weight loss from the TG curve is 12% from the temperature of 40˚C to103˚C, due to the elimination of water, carbon dioxide and nitrogen dioxide. In the DTA curve, two exothermic peaks are observed at 433˚C (sharp) and 570˚C (strong), respectively demonstrating the combustion of organic residuals in the matrix studied these strong exothermic peak at 433˚C in the DTA curve corresponds to the decomposition temperature of PVP is well above the heating temperature employed in the present work. No weight loss is observed above 550˚C, which indicates the completion of the decomposition process of PVP at this temperature. Correspondingly the weight loss in TG line is 18% between the temperatures from 470˚C to 600˚C [24].

DTA curves in **Figures 6(b)** show five exothermic peaks at 78˚C, 111˚C, 380˚C, 431˚C and 527˚C, respectively and three endothermic peaks at 90˚C, 397˚C & 484˚C, respectively. **Figures 6(b)** shows the sharp and strong exothermic peaks at 380˚C - 527˚C confirming the combustion of organic residuals. A strong exothermic peak at 380˚C, 431˚C in the DTA curve corresponds to the decomposition temperature of PVP is well above the heating temperature employed in the present work. **Figures 6(c)** shows the (DTA) exothermic peak at 81˚C, 216˚C, 440˚C, and 531˚C ware caused by the agglomera-

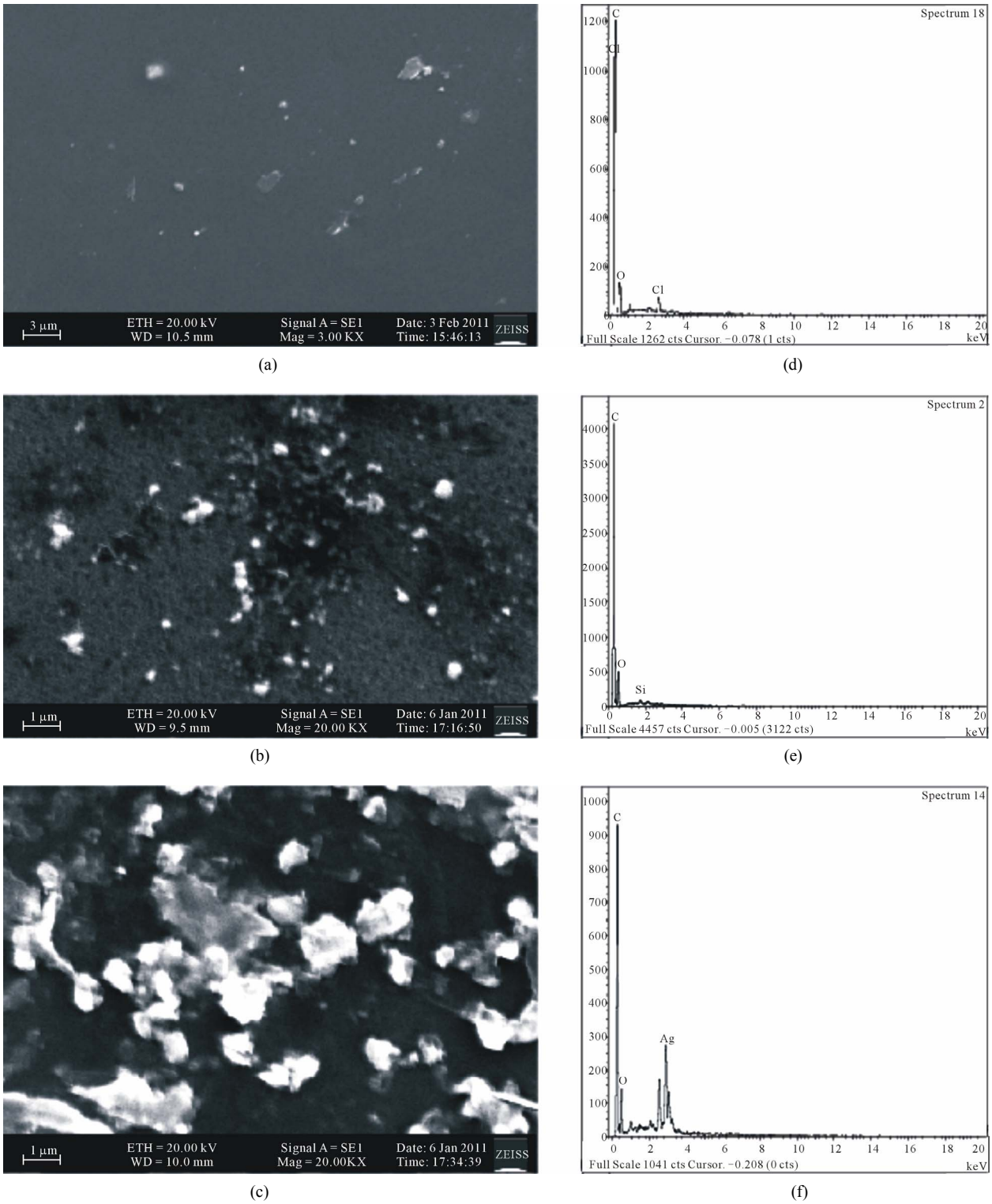

Figure 5. SEM Images and EDAX of ((a) & (d)) Host PVP, ((b) & (e)) Li^+: PVP and ((c) & (f)) Ag^+: PVP polymer films.

tion of silver particles and this strong exothermic peaks at 430˚C and 531˚C in the DTA curve corresponds to the decomposition temperature of PVP is well above the heating temperature employed in the present work respectively [25]. This shows that the thermal stability of the polymer is improved due to the presence of Ag as filler.

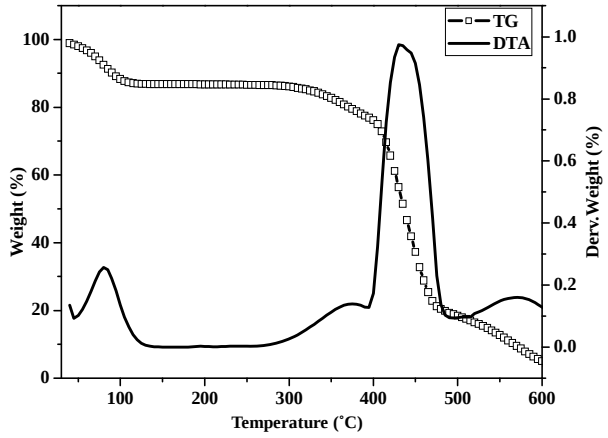

(a)

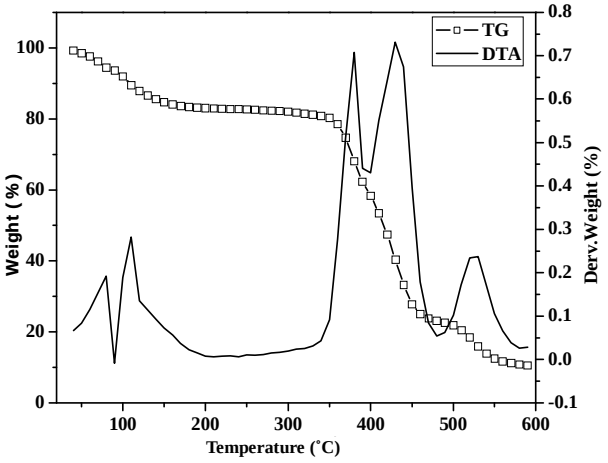

(b)

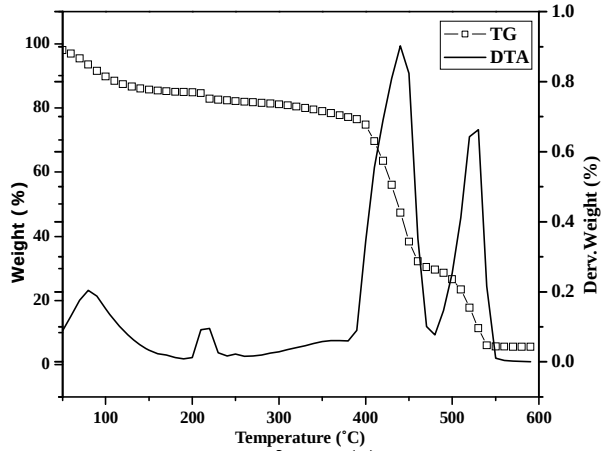

(c)

Figure 6. TG-DTA measurement of (a) Host PVP; (b) Li^+: PVP and (c) Ag^+: PVP polymer films.

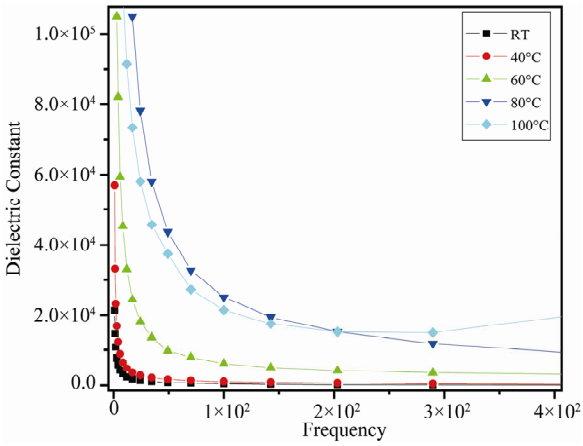

(a)

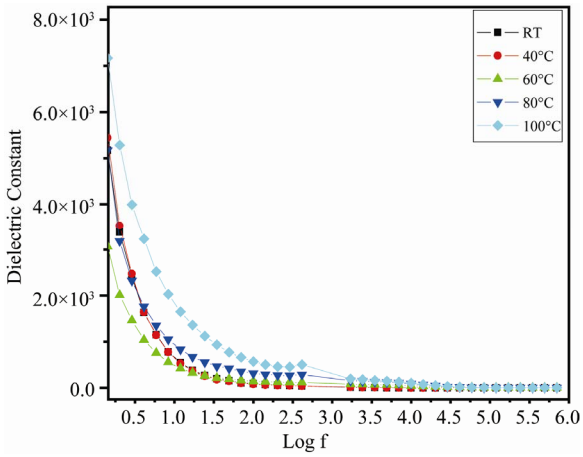

(b)

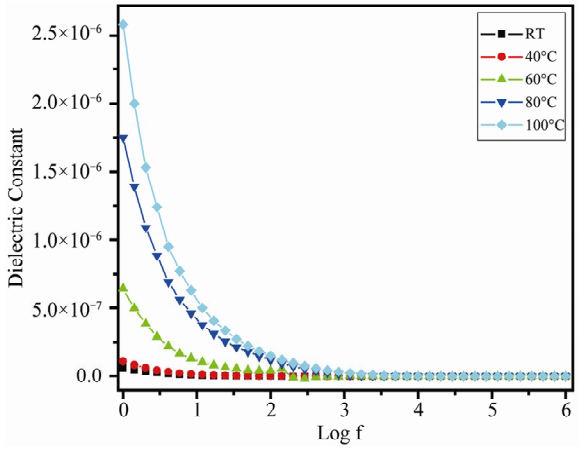

(c)

Figure 7. Dielectric Constant of (a) Host PVP; (b) Li^+: PVP and (c) Ag^+: PVP polymer films.

3.6. Dielectric Constant Analysis

Figures 7(a), **(b)** and **(c)** show the dielectric constant of the host PVP, Li^+: PVP and Ag^+: PVP polymer films at different temperatures as a function of frequencies by an Impedance Analyzer. The dielectric constant is inversely proportional to the frequency. This is a normal dielectric behavior that the dielectric constant decreases with an

increase in frequency. This can be understood on the basis that the mechanism of polarization [26].

3.7. Dielectric Loss Analysis

Figures 8(a), **(b)** & **(c)** show the dielectric loss tangent of the host PVP, Li^+: PVP and Ag^+: PVP polymer films at different temperatures as a function of frequencies by an Impedance Analyzer. This is a normal dielectric behavior of dielectric loss decreasing with an increase in frequency and it is understood on the basis of the mechanism of polarization [27].

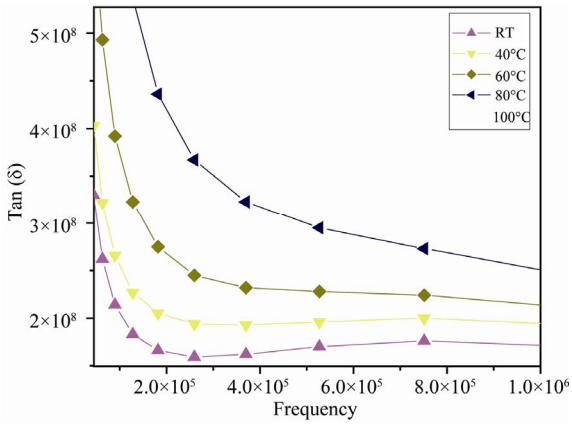

(a)

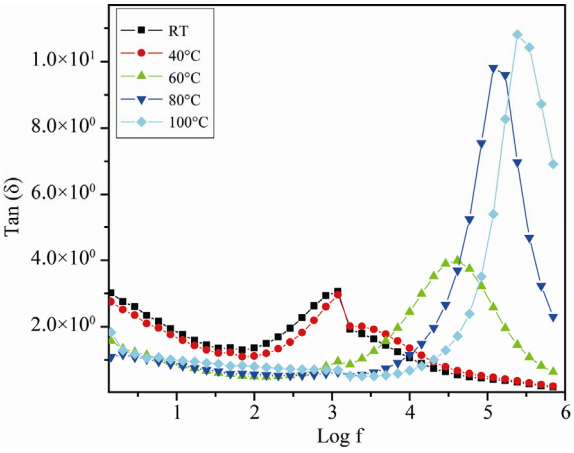

(b)

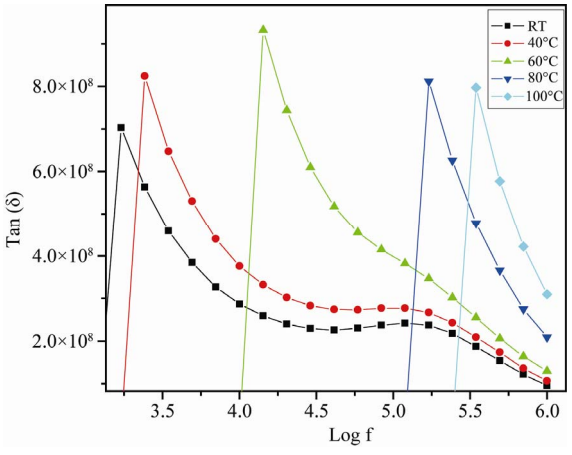

(c)

Figure 8. Dielectric Losses of (a) Host PVP; (b) Li^+: PVP and (c) Ag^+: PVP polymer films.

3.8. Cole-Cole Plots

The typical impedance plots (Z′ vs. Z″) for the host PVP, Li^+: PVP and Ag^+: PVP polymer films at different temperatures are shown in **Figures 9(a)**, **(b)** & **(c)** showing a high frequency semicircle and a low frequency spikes for Li^+: PVP and Ag^+: PVP polymer films doped polymer films. The plot consists of a low frequency spike, which is due to the effect of the blocking electrodes. The semicircles can be represented by a parallel combination of a capacitor, which are due to the immobile polymer chains and resistance, due to the mobile ions inside the polymer matrix. The bulk resistances for Li^+: PVP and Ag^+: PVP polymer films have been calculated from the low frequency spikes intercept of the spikes on the real axis [28]. The bulk resistance R_b decreases with an increase at different temperatures. Conductivity of the solid polymer electrolyte has been calculated from the measured bulk resistance. From **Figures 9(a)**, **(b)** & **(c)**, it is observed that the conductivity values of the completed systems do not show any abrupt jump with the temperature change, indicating that these polymer films exhibit a completely amorphous structure [29]. The increase in conductivity with temperature may be due to decrease in viscosity and hence increases the chain flexibility [30]. The increment of temperature causes the increase in conductivity due to the increased free volume and their respective ionic and segmental mobility.

The activation energies were calculated from logσ Vs 1000/T (**Figures 10(a)**, **(b)** & **(c)**) plots using the following Arrhenious equation.

$$\sigma = \sigma_0 \exp\left(\frac{-E_a}{kT}\right)$$

where σ_o is a constant, E_a is the activation energy, k is the Boltzmann constant and T is the absolute temperature. The slop gives the activation energy of the polymer films. The calculated activation energies of these polymers films are 3.8022 (Host PVP), 2.0678 (Li^+: PVP) and 2.9834 (Ag^+: PVP) respectively.

4. Conclusions

In summary, it could be concluded that transparent PVP, Li^+: PVP and Ag^+: PVP polymer films have successfully been synthesized in analyzing their structural, optical, thermal and electrical properties from the measurement of their XRD, FTIR, SEM images, EDAX, Absorption,

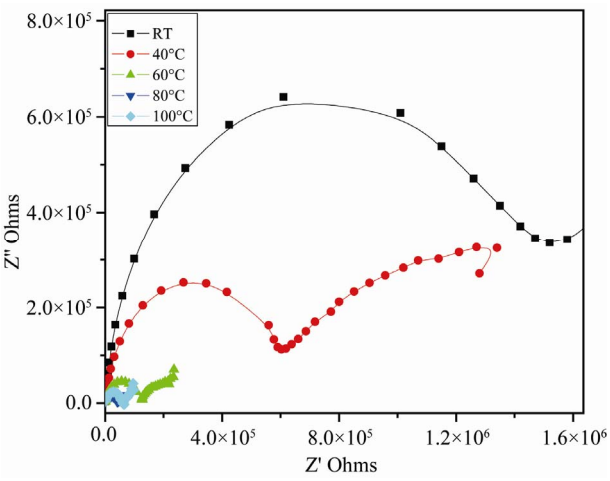

(a)

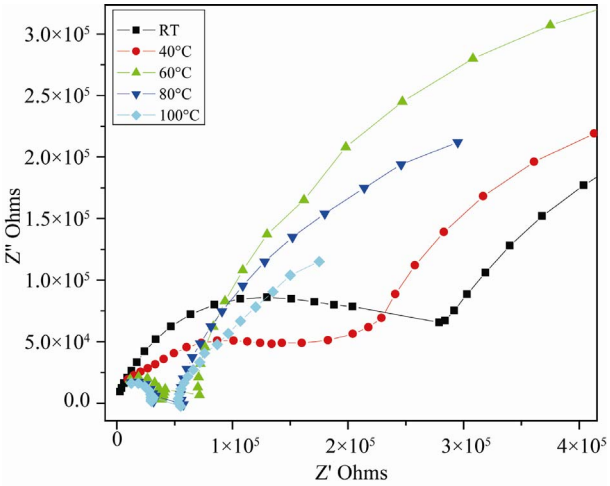

(b)

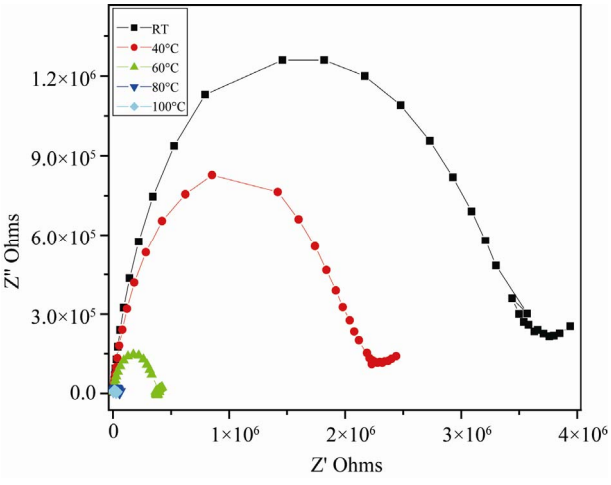

(c)

Figure 9. Cole-Cole plots of (a) Host PVP; (b) Li^+: PVP; (c) Ag^+: PVP polymer films.

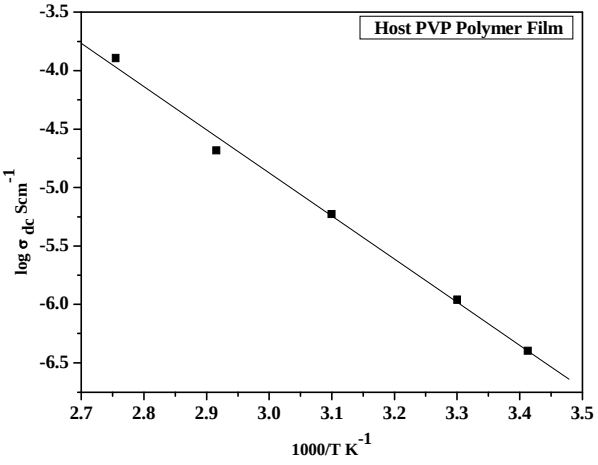

(a)

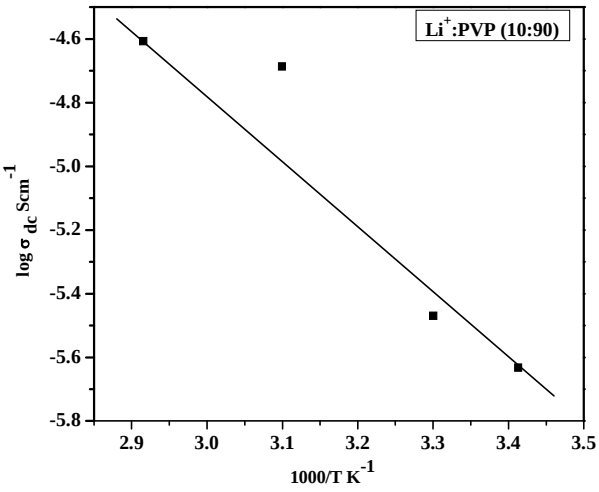

(b)

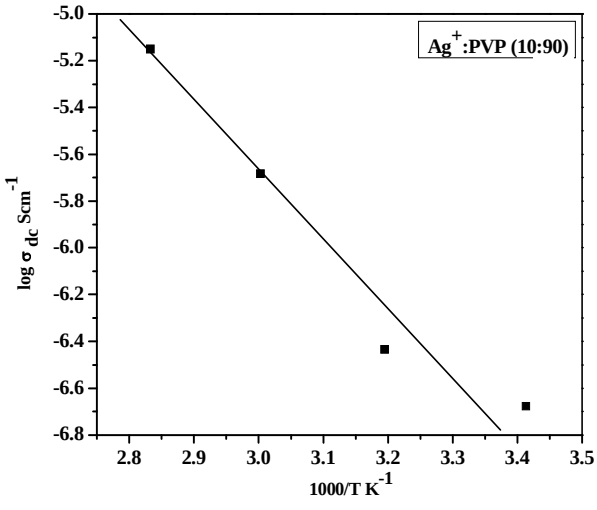

(c)

Figure 10. Arrhenius plots of (a) Host PVP; (b) Li^+: PVP; (c) Ag^+: PVP polymer films.

TG-DTA and Impedance Spectral profiles. The dielectric properties (dielectric constant (ε'), tanδ) of these films are showing a decreasing trend an increase in the frequency because of the occurrence of space charge polarization at the electrode-electrolyte interface. The impedance plots reveal that ionic conductivities of the reference PVP (1.57×10^{-4} S/cm), Li^+: PVP (8.55×10^{-3} S/cm) and Ag^+: PVP (1.03×10^{-3} S/cm) polymer films were calculated from bulk resistance, which varies with temperature. On comparison of results it is noticed that Li^+: PVP polymer film has shown an enhancement in conductivity besides its mechanical strength and therefore Li^+: PVP electrolytes could be found to be more suitable for their potential applications in the progress of battery materials and ionic devices.

REFERENCES

[1] M. J. Reddy, S. S. Rao, E. L. and U. V. S. Rao, "Study of a Thin Film Electrochemical Cell Based on (PVP + AgNO) Electrolyte," *Solid State Ionics*, Vol. 80, No. 1-2, 1995, pp. 93-98. doi:10.1016/0167-2738(95)00128-S

[2] Z. T. Rui, L. Ran, L. L. Xin, Z. Y. Ying, L. T. Jin and Y. J. Nian, "Photochromic Polyoxotungstoeuropate K12 [Eu P5W30O110]/Polyvinylpyrrolidone Nanocomposite Films," *Journal of Solid State Chemistry*, Vol. 172, No. 2, 2003, pp. 458-463. doi:10.1016/S0022-4596(03)00036-7

[3] C. S. Ramya, S. Selvasekarapandian, G. Hirankumar, T. Savitha and P. C. Angelo, "Investigation Sonthe Effect of Complexation of NaFsalt with Polymerblend (PEO/PVP) Electroly Tesonionic Conductivity and Optical Energy-bandgaps," *Journal of Non-Crystal Solids*, Vol. 354, 2008, pp. 1494-1502. doi:10.1016/j.jnoncrysol.2007.08.038

[4] J. Zhang, H. Liu, Z. Wang and N. Ming, "Low-Temperature Growth of ZnO with Controllable Shapes and Band Gaps," *Journal of Crystal Growth*, Vol. 310, No. 11, 2008, pp. 2848-2853. doi:10.1016/j.jcrysgro.2008.02.014

[5] H. Fatima, T. Sandrine, M. Gilles and G. Jean-Luc, "Photooxidation of Poly (N-vinylpyrrolidone) (PVP) in the Solid State and in Aqueous Solution," *Polymer Degradation and Stability*, Vol. 94, No. 12, 2009, pp. 2257-2266. doi:10.1016/j.polymdegradstab.2009.08.007

[6] Y. Kobayashi, A. Kosuge and M. Konno, "Fabrication of High Concentration Barium Titanate/Polyvinylpyrrolidone Nano-Composite Thin Films and Their Dielectric Properties," *Applied Surface Science*, Vol. 255, No. 5, 2008, pp. 2723-2729. doi:10.1016/j.apsusc.2008.08.006

[7] C. Hsien-Wei, L. Tzu-Pin and C. Feng-Chih, "Ionic Conductivity Enhancement of the Plasticized PMMA/$LiClO_4$ Polymer Nanocomposite Electrolyte Containing Clay," *Polymer*, Vol. 43, No. 19, 2002, pp. 5281-5288. doi:10.1016/S0032-3861(02)00339-7

[8] R. Baskarana, S. Selvasekarapandiana, N. Kuwatab, J. Kawamurab and T. Hattori, "Structure, Thermal and Transport Properties of PVAc-$LiClO_4$ Solid Polymer Electrolytes," *Journal of Physics and Chemistry of Solids*, Vol. 68, No. 3, 2007, pp. 407-412.

[9] S. Vaidyanathan, N. Nicholas, E. G. Seebauer, A. Mark, R. Shannon and I. Masel, "Synthesis and Characterization of Polyvinylpyrrolidine Assisted Tantalum Pentoxide Films," *Thin Solid Films*, Vol. 516, No. 15, 2008, pp. 4784-4792. doi:10.1016/j.tsf.2007.08.138

[10] L. Katarzyna, "Miscibility and Interactions in Chitosan acetate/Poly (N-Vinylpyrrolidone) Blends," *Thermochemica Acta*, Vol. 517, No. 1-2, 2011, pp. 90-97.

[11] X. L. Liu, K. Han, M. Gu, S. M. Huang, B. Liu and N. Chen, "Optical Properties of $GdTaO_4$:Eu^{3+} Thick Films Prepared from a PVP-Containing Solution," *Applied Surface Science*, Vol. 255, No. 8, 2009, pp. 4680-4683. doi:10.1016/j.apsusc.2008.12.026

[12] R. Nithya and R. Ragunathan, "Synthesis of Silver Nanoparticle Pleurotus Sajor Caju and Its Antimicrobial Study," *Digest Journal of Nanomaterials and Biostructures*, Vol. 4, No. 4, 2009, pp. 623-629.

[13] V. P. Ghodake, P. T. Kininge, S. P. Magdum, A. S. Dive and M. M. Pillai, "Bipsynthesis of Silver Nanoparticles Using Trichosporon Beigelii Ncim 3326 and Evaluation of Their," *Journal of Engineering Research and Studies*, Vol. 11, No. 1, 2011, pp. 32-36.

[14] L. Manhong, Y. Xiaoping, L. Hanfan and Y. Weiyong, "An Investigation of the Interaction between Polyvinylpyrrolidone and Metal Cations," *Reactive & Functional Polymers*, Vol. 44, No. 1, 2000, pp. 55-64. doi:10.1016/S1381-5148(99)00077-2

[15] E. K. Elumalai, "Extracellular Synthesis of Silver Nanoparticles Using Leaves of *Euphorbia hirta* and Their Antibacterial Activities," *Journal of Pharmaceutical Sciences and Research*, Vol. 2, 2010, pp. 549-554.

[16] S. S. Gasaymeh, S. Radiman, L. Y. Heng and E. G. H. M. Saion, "Synthesis and Characterization of Silver/Poly- vinilpirrolidone (Ag/PVP) Nanoparticles Using Gamma Irradiation Techniques," *American Journal of Applied Sciences*, Vol. 7, No. 7, 2010, pp. 892-901. doi:10.3844/ajassp.2010.892.901

[17] M. P. Zheng, M. Y. Gu, Y. P. Jin and G. L. Jin, "Optical Properties of Silver-Dispersed PVP Thin Film," *Materials Research Bulletin*, Vol. 36, No. 5-6, pp. 2001, 853-859.

[18] Y. Z. Wang, Y. X. Li, S. T. Yang, G. L. Zhang, D. M. An, C. Wang, Q. B. Yang, X. S. Chen, X. B. Jin and Y. Wei, "A Convenient Route to Polyvinyl Pyrrolidone/Silver Nanocomposite by Electrospinning," *Nanotechnology*, Vol. 17, No. 13, 2006, pp. 3304-3307. doi:10.1088/0957-4484/17/13/037

[19] R. Geethalakshmi and D. V. L. Sarada, "Synthesis of Plant-Mediated Silver Nanoparticles Using *Trianthema decandra* Extract and Evaluation of Their Anti Microbial Activities," *International Journal of Engineering Science and Technology*, Vol. 2, No. 5, 2010, pp. 70-975.

[20] H.-D. Wu, *et al.*, "The Interaction Behavior of Polymer Electrolytes Composed of Poly (Vinyl Pyrrolidone) and Lithium Perchlorate ($LiClO_4$)," *Polymer*, Vol. 42, No. 2, 2001, pp. 555-562.

doi:10.1016/S0032-3861(00)00213-5

[21] A. T. Donald, M. Taketoshi, F. Akira, *et al.*, "Large-Scale Fabrication of Ag Nanoparticles in PVP Nanofibres and Net-Like Silver Anofibre Films by Electrospinning," *Nanotechnology*, Vol. 18, 2007, pp. 1-7.

[22] X. K. Mengy, S. C. Tang and S. Vongehr, "A Review on Diverse Silver Nanostructures," *Journal of Material Science and Technology*, Vol. 26, No. 6, 2010, pp. 487-522. doi:10.1016/S1005-0302(10)60078-3

[23] C. Misuk, *et al.*, "One-Step Synthesis of Polymer-Stabilized Ag Particles on PEDOT: Effects of Stabilizer and Electrochemical Method on Formation of Ag Particle," *Macromolecular Research*, Vol. 18, No. 11, 2010, pp. 1070-1075.

[24] Z. Cui, H. Ren, G. Liu and G. Hong, "Synthesis and Characterization of Terbium-Trimesic Acid Luminescent Complex in Polyvinylpyrrolidone Matrix," *Journal of Rare Earths*, Vol. 24, No. 6, 2006, pp. 724-727. doi:10.1016/S1002-0721(07)60016-7

[25] S. G. Shawkat, R. Shahidan, Y. H. Lee and S. Elias, "Gamma Irradiation Synthesis and Influence the Optical and Thermal Properties of Cadmium Sulfide (CdS)/Poly (Vinyl Pyrolidone) Nanocomposites," *American Journal of Applied Sciences*, Vol. 7, No. 4, 2010, pp. 500-508. doi:10.3844/ajassp.2010.500.508

[26] M. Prabu, S. Selvesekarpanddian, A. R. Kulkarni, S. Karthikeyan and G. S. Structural, "Dielectric and Conductivity Studies of Yettrium-Doped $LiNiPO_4$ Hirankumar, and C. Anjeevi Raj," *Ionics*, Vol. 17, 2011, pp. 201-207. doi:10.1007/s11581-011-0535-5

[27] D. Supti and J. A. Bhattacharyya, "Dielectric Relaxation Spectroscopy for Evaluation of the Influence of Solvent Dynamics on Ion Transport in Succinonitrile-Salt Plastic Crystalline Electrolytes," *Journal of Physical Chemistry B*, Vol. 115, No. 10, 2011, pp. 2148-2154. doi:10.1021/jp108848b

[28] R. J. Sengwa, S. Choudhary and S. Sankhla, "Low Frequency Dielectric Relaxation Processes and Ionic Conductivity of Montmorillonite Clay Nanoparticles Colloidal Suspension in Poly (Vinyl Pyrrolidone)-Ethylene Glycol Blends," *Express Polymer Letters*, Vol. 2, No. 11, 2008, pp. 800-809. doi:10.3144/expresspolymlett.2008.93

[29] M. H. Bhat, M. Kandavel, M. Ganguli and K. J. Rao, "Li^+ Ion Conductivities in Boro-Tellurite Glasses," *Bulletin of Materials Science*, Vol. 27, No. 2, 2004, pp. 189-198. doi:10.1007/BF02708504

[30] M. Vijayakumwr, S. Selvesekarpanddian, D. Jayanthi and R. Kavitha, "Effect of Annealing on Li_2O-TiO_2-V_2O_5 Electrolyte Materials," *Solid State Ionics*, Vol. 154, 2002, pp. 773-777. doi:10.1016/S0167-2738(02)00703-8

